Spring 2015

Magnetic manipulation and multimodal imaging for single cell direct mechanosensing

Robert L. Wilson
Purdue University

Graduate School Form 30
Updated 1/15/2015

PURDUE UNIVERSITY
GRADUATE SCHOOL
Thesis/Dissertation Acceptance

This is to certify that the thesis/dissertation prepared

By Robert L. Wilson

Entitled

Magnetic Manipulation and Multimodal Imaging fof Single Cell Direct Mechanosensing

For the degree of Master of Science in Biomedical Engineering

Is approved by the final examining committee:

Dr. Corey P. Neu
Chair

Dr. Sarah Calve

Dr. Craig Goergen

To the best of my knowledge and as understood by the student in the Thesis/Dissertation Agreement, Publication Delay, and Certification Disclaimer (Graduate School Form 32), this thesis/dissertation adheres to the provisions of Purdue University's "Policy of Integrity in Research" and the use of copyright material.

Approved by Major Professor(s): Dr. Corey P. Neu

Approved by: George R. Wodika 3/5/2015

Head of the Departmental Graduate Program Date

MAGNETIC MANIPULATION AND MULTIMODAL IMAGING FOR SINGLE CELL DIRECT MECHANOSENSING

A Thesis

Submitted to the Faculty

of

Purdue University

by

Robert L. Wilson

In Partial Fulfillment of the

Requirements for the Degree

of

Master of Science in Biomedical Engineering

May 2015

Purdue University

West Lafayette, Indiana

ACKNOWLEDGEMENTS

As my time as a master student comes to a close, there seems to be an endless number of people to thank for their advice and patience. First, I would like to thank Dr. Corey Neu for all of his help and guidance on this thesis project. He has aided me in my thought process as a researcher and increased my aptitude as an independent thinker, making me a better engineer.

I'd like to give a special thank you to Drs. Charilaos Mousoulis and Xin Xu for their help on this project in both the understanding of the 'nano' world and the creation and application of my magnetic manipulation method. I would also like to say a big thank you to Dr. Jonathan Henderson for allowing me to pester him with various questions almost constantly throughout my studies. I have truly learned a lot with your help. Additionally, Id like to thank my fellow lab members (Tyler Novak, Kateri Fites M.S., Ben Seelbinder, Logan Worke, Luyao Cai, Celina Twitchell, Benjamin Seelbinder, and Matt Thompson) for all of their help as well as all of my other friends I have made in my time at Purdue. You have made the experience unforgettable.

Lastly, my final and greatest thank you goes to my family. Without their support, I would not be where I am today. It is with their encouragement and support that I dare to create and design as an engineer to further human knowledge and better the human condition.

This work was supported by grants from the NSF (CMMI 1100554 and CMMI 1349735) and NIH (R01 AR063712 and R21 AR064178).

TABLE OF CONTENTS

Page

Page

ABSTRACT

Wilson, Robert L. M.S.B.M.E., Purdue University, May 2015. Magnetic Manipulation and Multimodal Imaging for Single Cell Direct Mechanosensing. Major Professor: Corey P. Neu.

The study of internal mechanics of single cells is paramount to understand mechanisms of mechanoregulation. External loading and cell-mediated force generation result in changes in cell shape, rheology, and the deformation of subcellular structures such as the nucleus. Moreover, alterations in the processes that regulate these responses have been further correlated to specific pathologies. Cellular deformation is often studied through application of forces in the environment of the cell, relying on strain and stress transfer through focal adhesions and the cytoskeletal system. However, the transfer of these external forces to internal mechanics can introduce uncertainties in the interpretation of subcellular responses. Our group has focused on minimally-invasive techniques for the study of internal mechanical perturbation and mechanobiology measures. We have been particularly interested in multimodal imaging methods that combine and leverage nano-scale spatial localization, visualization, biophysical and physico-chemical analysis

features to reveal information that cannot be attained by any single method alone. We recently fabricated novel atomic force microscopy (AFM) cantilevers, functionalized to generate small, highly-localized magnetic fields, for the controlled force application and sensing of single cells. In combination with AFM and fluorescence microscopy detection capabilities, this technique enables the selective stimulation and monitoring of cells injected with superparamagnetic microbeads. Though the targeted magnetic force application, we are able to apply various waveforms to direct the microdisplacements of the injected beads to allow insight into the structural architecture of the cell. Coupling this with AFM techniques further yields insight into internal and external mechanics over time. This technique can be extended to include studies of intranuclear strain dynamics through fluorescent labeling of specific cellular targets and image post-processing algorithms such as hyperelastic warping. Furthermore, the ability to alter the culture environment (e.g. to manipulate osmotic pressure or enable drug delivery) allows this technique to be a powerful single cell analysis tool for a diverse set of applications. We demonstrate the feasibility of this technique through the localized application of low magnetic fields that produce bead displacements in the micrometer scale. The effects of larger induced magnetic fields in the displacement field are also presented, along with validation and viability studies, and a range of practical applications for the study of single cells.

CHAPTER 1. MAGNETIC MANIPULATION AND MULTIMODAL IMAGING FOR SINGLE CELL DIRECT MECHANOSENSING

Abstract

Objectives:

1. To demonstrate the feasibility of magnetic manipulation by an atomic force microscopy (AFM) inductor enabled microcoil technique through the characterization and localized application of low magnetic fields that produces nanometer sized bead displacements.

2. To increase the detail, amount of data, and overall throughput produced by magnetic manipulation through the AFM inductor enabled microcoil technique to be able to tease apart variability in cellular response.

Methods: The characterization of the magnetic field strength was calculated. Primary chondrocytes were injected with 1 μm superparamagnetic and nonmagnetic carboxylate microparticles. The cells were subjected to a localized magnetic field through a micro-inductor enabled AFM cantilever tip. Analysis of particle displacement was ran via local thresholding coupled with centroid tracking.

Results: The microcoil magnetic field was found to be in the femtonewton (fN) scale when a 0.2mA current was applied 10-30μm away. This produced significant differences

in bead movement between the magnetic and nonmagnetic beads. When the magnetic field was applied, the superparamagnetic beads displaced 33 ± 13nm as compared to 3 ± 8nm for the nonmagnetic beads, prompting a continuation of these studies with a confocal microscope. Testing with higher temporal resolution confirmed the previous findings.

Conclusions: This technique paves the way for a variety of high throughput single cell analysis studies. With an increase in temporal resolution and the addition of 3-D imaging, this will be useful for studies into cellular rheology. Additionally, more insight into the mechanobiological stress and strain transfer can be examined.

1.1. Introduction

The study of internal mechanics of single cells is paramount to understand mechanisms of mechanoregulation. External loading and cell-mediated force generation result in changes in cell shape, rheology, and the deformation of subcellular structures such as the nucleus.[1] Moreover, alterations in the processes that regulate these responses have been further correlated to specific pathologies such as heart failure and atherosclerosis. Consequently, there are numerous methods for studying these processes.[2] Cellular deformation is often studied through application of forces in the environment of the cell, relying on strain and stress transfer through focal adhesions and the cytoskeletal system. Methods such as optical tweezers, magnetic tweezers, and atomic force microscopy (AFM) have the ability to noninvasively study the cytoskeleton directly.[3] Optical tweezers rely on the ability to optically “trap” the bead or beads in

question by lasers.[4] This method, while useful, is not ideal for submerged studies due to the diffraction of the light due to impurities in solutions such as cell media.[3] Pioneered by Crick et. al. 1948, magnetic tweezers or microrheology allows for studies of cell responses and rheology.[5]–[13] When utilizing an electromagnetic magnetic field in this traditional fashion all magnetic beads are affected, thus introducing confounding effects such as initial cell response and negating any reusability.

The magnetic tweezers setup was improved to include microns of displacement in both the x and y directions.[14] Approaches were taken to improve the throughput of this testing modality. By wrapping the magnet either around a probing rod or an offset mount, the affected area decreased considerably. However, there is still a large area affected. With todays imaging modalities, it is possible to run a magnetic tweezer setup to analyze movement on increasingly smaller scales, such as the nucleus[7][9]. With these large areas of magnetic application, there is an inherently low throughput tradeoff between imaging resolution/magnification and sample size. As scientific discovery approaches smaller scales, the classic application of magnetic tweezers becomes less efficient. In order for this approach to stay viable in this transition, a fundamental change in approach must be made.

Atomic Force Microscopy (AFM) is a traditional approach to locally monitor single cell characteristics on the micro to nanoscale level. The standard application is to locally externally probe cells and extrapolate stiffness characteristics from the induced cantilever deflection.[15]–[18] The inherent local testing property of this modality has allowed it to become a frontrunner in noninvasive mechanical characteristics of single cells. Yet, it gives no direct measurements of internal mechanics. However, with recently

developed micro-inductor enabled cantilevers, it is possible to merge the fields of AFM and magnetic tweezers thus providing a local system to analyze internal and external mechanics on these smaller scales while keeping a high thoughput of testing.

Here we present the validation study for this locally applied magnetic tweezer setup as well as the resulting microparticle displacements. The objectives are to first create and sense magnetic bead movement on a fine nanometer scale while still keeping a high throughput, then provide detailed analysis from these tests. Cells were injected with superparamagetic beads. The micro inductor enabled cantilever was brought with in 15um above the cells. A magnetic field was induced on the femtonewton scale. This produced nanometer sized displacements of the magnetic beads, which could be correlated to cytoplasmic mechanics. To the best of our knowledge, this is the first time use of AFM as a local 3-D magnetic tweezer approach.

1.2. Methods

1.2.1. Overview

Cells were ballistically injected with magnetic and nonmagnetic beads. These cells were then subjected to local magnetic fields. The movement of these beads due to this magnetic field was tracked and analyzed.

1.2.2. Calculation of Magnetic Field Strength

The forces applied to the superparamagnetic beads were estimated using the standard formula for weak magnetic fields [19]:

$$\vec{F} = (\vec{m}_{bead} \cdot \nabla)\vec{B} = \rho V(\vec{M}_0 \cdot \nabla)\vec{B} + \frac{V\chi_{bead}}{\mu_0}(\vec{B} \cdot \nabla)\vec{B} \qquad (1)$$

where V is the volume of the magnetic beads (3.82e-19m^3), χ_{bead} is the magnetic susceptibility of the beads, (0.17, supplied by manufacturer), $\mu_0 = 4\pi\times10^{-7}(TmA^{-1})$, the permeability of a vacuum. From Figure 1d, $\vec{B}$ at 10-30um is 1.3e-5T with a center gradient $\frac{dB}{dxz}$ of .31$\frac{T}{m}$, resulting in single femtonewton (fN) forces.

1.2.3. Cell Culture

Primary Chondrocytes:

Primary Chondrocytes were harvested from the lateral and medial femoral condyles of five- to seven-month-old bovine knees. The femur was isolated and tissue samples removed via scalpel. The tissue was degraded in 50mL Colagenase-P (Life Technologies, Carlsbad, CA) for 3 hours. The solution was run through a 70μm strainer (Life Technologies). The cells were resuspended in Dulbecco's modified Eagle's medium (DMEM/F12) and plated. Cells were cultured (37^{o}C, 5% CO_2) in Dulbecco's modified Eagle's medium (DMEM/F12) supplemented with 10% fetal bovine serum (FBS), 0.1%

bovine serum albumin, 50 ug/ml L-Ascorbate-2-phosphate, 100 units/mL penicillin, and 100 ug/mL streptomycin (Life Technologies, Carlsbad, CA).

1.2.4. Ballistic Injection of Microparticles

Primary Chondrocytes for Widefield Studies:

Fluorescent superparamagnetic beads (0.9μm; excitation/emission: 480nm/520nm or 660nm/690nm; Bangs Labs, Fishers, IN) and carboxylate beads (1.1μm; excitation/emission: 580nm/605nm; Life Technologies) were prepared (at 120μg/ml) in DI water. Two 35mm petri dishes were plated with 1.5 million cells each and allowed to sit for no less than 3 hours. The media was then removed, and the microparticles were ballistically injected (35% injection rate; 1350 psi; Biolistic PDS-1000/HE, BioRad, Richmond, CA) into the cytoplasm or nucleus of the cells (Figure 2a). The cells were incubated for 8-24 hours, released (TrypLE Express^{TM}; Life Technologies) and suspended together, and then replated on 35mm Cellview^{TM} cell culture dishes (Greiner Bio-One, Frickenhausen, Germany). After a 1-hour equilibration, chondrocytes were washed with medium and stained with Hoechst and Calcein AM (Life Technologies) prior to imaging allowing the fluorescence of the nucleus and cytoplasm respectively. Confocal microscopy (Figure 2b; AIR_MP, Nikon) confirmed the penetration of the microbeads into the cytoplasm and nuclei.

Primary Chondrocytes for Confocal Studies:

Fluorescent superparamagnetic beads (0.9μm; excitation: 660nm emission: 690nm; Bangs Labs, Fishers, IN) and carboxylate beads (1.1μm; excitation: 580nm emission: 605nm; Life Technologies) were prepared (at 120μg/ml) in DI water. A 35mm petri dish was plated with 1.5 million cells and allowed to sit for no less than 3 hours. The media was then removed, and the microparticles were ballistically injected (1350 psi; Biolistic PDS-1000/HE, BioRad, Richmond, CA) into the cytoplasm or nucleus of the cells. The cells were incubated for 8-24 hours, released (TrypLE Express^{TM} for Primary Chondrocytes, 0.5% Trypsin/EDTA for HT-1080 LifeAct^{TM}–TagGFP2, Life Technologies) then replated onto a 35mm Cellview^{TM} cell culture dish (Greiner Bio-One, Frickenhausen, Germany). After an hour equilibration, the cells were washed with DMEM and stained with Hoechst (Life Technologies) prior to imaging.

1.2.5. Magnetic Manipulation

Widefield Microscope Studies:

AFM Cantilevers were created utilizing soft lithography techniques resulting in planar microcoils of silicon nitride coated in Parylene-C. Microbead movements were accomplished using a 2 turn microcoil and custom AFM nosecone that was immersed in media and lowered to within 10-30 um of the chondrocyte monolayer (Figure 1a-c and

Figure 3a-c). A current pulse (0.2mA, 0.5s, 0.1 Hz) was passed to the microcoil by a function waveform generator (Agilent). Cells were simultaneously imaged using widefield microscopy (Eclipse Ti, Nikon) and a CCD camera (iXon+, Andor, Belfast, NIR) for 60s undisturbed, 120s with pulsing, and a final 120s minutes undisturbed, at high spatiotemporal resolution (Figure 3d-f, 180nm/px, 1.2s frame rate).

Confocal Microscope Studies:

4 turn microcoils were utilized for testing by confocal microscopy. A microcoil was lowered to 10-30 μm above the cells in the same manner but with the system mounted on a confocal microscope (A1R MP, Nikon). Testing was performed over 15 seconds (5s off, 5s pulsing, 5s off) and 5 min (same parameters as widefield microscopy testing) standardized protocols. Imaging was achieved with a 0.2s and 55nm/px temporal resolution and spatial resolution respectively.

1.2.6. Image Analysis

Ballistic Injection Quantification:

Image stacks were separated into individual channels. Magnetic and nonmagnetic bead channels were combined and made into a binary mask. The cytoplasm channel was altered into an inverse binary mask. The two binary images were subtracted from one another leaving just particles that were directly over the cytoplasm (i.e. were injected into cells). These particles were counted via ImageJ. Lastly, the nuclei were counted for a

total number of cells. Dividing the injected particle count by cell count results in an estimate of total cells injected (Figure 2c-g).

Widefield Microscope Studies:

Microbead positions were analyzed using semiautomated threshold and particle centroid-tracking routines (ImageJ and MATLAB The Mathworks, Natick, MA) with a 15nm spatial resolution [20]). The particle mean displacements (MDs) were equated overtime (Figure 4a). The MDs were binned into 30s increments yielding average centroid movements. The MDs were then offset to the first 30s of Brownian motion. (Figure 4b, n=27)

Confocal Microscope Studies:

Microbead positions were first analyzed using a semiautomated threshold and particle centroid-tracking routines. The Mean Squared Displacements (MSDs) of all particles were then refit by the Levenberg-Marquardt 2-D Gaussian particle tracking method via the ImageJ plug-in Particle Track and Analysis (PTA) by Yoshiyuki Arai. MSDs were calculated for the 15s test and then binned to every 2.5s (Figure 5a). The 5 minute test MSDs were baselined to their average 30s of displacement. All displacements were then binned into 30s bins and averaged together for each particle type for average MSDs (Figure 5d, n = 35). All particles were separated into groups determined by their relative position to the microcoil, either directly under the first two turns (refered to as the “inner” section) or under the outer two turns (referred to as the “outer”, Figure 5b-c). Nuclear

movement was also assessed through a binary threshold and particle centroid tracking code, yielding average movement of nuclei during testing. However, the standard deviation was incredibly large due to low imaging signal and was not quantified.

1.2.7. Statistical Analysis

Data was analyzed by means of a two-factor analysis of variance (ANOVA). The Magnetic property (superparamagnetic and nonmagnetic) and time were treated as categorical data, with mean displacements of the microparticles as the dependent variable. The magnetic field application is embedded in the time course series. Additionally, the significance of an interaction term between magnetic properties and time was calculated (Minitab, State College, PA) Results were found to be significant if $p<0.05$.

1.3. Results

1.3.1. Widefield Magnetic Manipulation Testing

Applied magnetic fields from 2 turn hybrid microcoils resulted in motion of superparamagnetic microbeads, but not nonmagnetic beads, as quantified by the MDs over time. (Figure 4). A two-way ANOVA of magnetic particles vs. nonmagnetic particles overtime shows significance of bead properties and magnetic field application ($p<0.05$ for magnetic, time, and the interaction term.) It is important to note that at 0.2mA

heat production is at a biologically relevant temperature between 20-30℃ with a negligible coil deflection (data not shown, personal communication from Dr. Charilaos Mousoulis)

1.3.2. Confocal Magnetic Manipulation Testing

The 15 second tests yielded no significant movement of the embedded magnetic beads (Figure 5a). However, magnetic forces applied from 4 turn hybrid microcoils during the 5 min tests resulted in significant motion of superparamagnetic microbeads compared to nonmagnetic beads, as quantified by the MSDs over time (Figure 5d). Data was offset to mean sample drift overtime (Figure 5c). There is a difference in magnitude of response based on the location of the magnetic beads relative to the turns of the coil. The beads directly below the inner two turns of the coil move significantly more than those directly below the outer two turns (Figure 5b-c).

1.4. Discussion

Magnetic tweezer studies of single cells are classically conducted with high pico- to nanonewton forces resulting in micron-scale displacement of intracellular particles.[6] However, single molecule studies can be done at lower forces producing nanometer sized displacements, suggesting that lower intracellular forces may cause displacements.[3] Additionally this low field yields itself well to the potential for isolated single molecule studies. As the scientific community migrates to smaller *in vivo* and *in vitro* studies, a

method to produce and study the results of these small forces must be created. Here, we have demonstrated that magnetic fields acting on the superparamagnetic beads generated femptonewton-scale forces and nanoscale displacements on beads embedded in the cytoplasm of cells with a range of cytoskeletal strength (Figure 4b and Figure 5d). The final displacement graphs show significant movement of these beads as compared to the nonmagnetic proving the feasibility of this method.

Interestingly, for the widefield microscopy studies, the post-pulse section moved 14nm more than the control of the same time period demonstrating the well-known microbead movement in the cytoplasm post magnetic field application.[9] However, the data suggests no recovery to original position. This could suggest active movement by the cell such as cytoskeletal remodeling. While the results from the widefield microscopy studies were promising, there was a high variability in individual results, as evidenced by the high standard deviation, that lead to further exploration. There are a number of reasons for the possible variability due to the small amount of movement that is produced and measured. As primary chondrocytes grow from passage to passage, they begin to differentiate into fibroblasts. The transformation causes the cytoskeletal stiffness to increase.[21] Widefield microscopy tests were conducted with passage 0 through passage 4 primary chondrocytes; the increase in stiffness alone could be enough to cause this difference in responses between tests. However, the specific passage of the primary chondrocytes for each test was not recorded. Nevertheless, it is a factor that can be controlled.

The cytoskeletal actin network is also a suspect for the nonuniform microparticle displacement.[22] Depending on the embedded location of the microparticle, the highly dynamic heterogeneous nature actin network could produce a significant variable effect. A typical actin filament is has a tensile strength of 108 ±5pN.[23] While the microparticles should not be directly bound to the actin filaments, if the microparticle were embedded into a dense region of actin, it would seem logical that it would require a stronger force to displace it.

Coil position relative to the microbeads is another proposed mechanism of variability. Since the magnetic field gradient is relative to the center of the coil, the actual field strength applied on the bead is nonuniform as a function of position in all three dimensions. The magnetic field gradient change in $\frac{dB}{dz}$ alone ($.31\frac{T}{m}$) could play a significant role (Figure 1d). At such low magnetic field strengths, these little changes can propagate to large differences in displacements.[19]

Due to the numerous potential causes of variability in response, a second set of studies were necessary to attempt to tease apart these responses. By using confocal microscopy, we were able to reduce a few of these variables. The z-slice sectioning of confocal microscopy is finer than a widefield system thus helping with our noise. The temporal and spatial resolution increased from 1.2s to .267s and 180nm/px to 55nm/px respectively. In order to keep the temporal resolution at a maximum, it was not possible to track the z position as a function of time using a confocal z stack. For additional variable control outside of the microscope system, only passage 4 primary chondrocytes were used.

Initially, fifteen-second tests were conducted. Due to the increase in temporal resolution, that was enough time to capture a sufficient amount of images for analysis. Upon analysis of this data, it was seen that there was no significant movement of these particles (Figure 5a). This suggests that the movement is subtle enough that the pulsing overtime eventually pulses the bead free of it actin network, but five seconds of pulsing is not enough. Perhaps the actin network is initially stronger than the fN forces created by the microcoil. It is apparent by looking at the full time course data (Figure 4b) that a single pulse is not enough to elicit a movement and response curve of a microparticle. However, gentle pulling overtime could coerce the bead from its actin-embedded position by magnetic manipulation. This prompted longer time course studies.

Five-minute tests were used to keep a consistency through the widefield and confocal testing data. The averaged and binned data shows that the magnetic beads do move significantly more than the nonmagnetic beads over time on the same scale as the widefield studies (Figure 5d). Interestingly, we also documented movement of the nonmagnetic beads over time. There is drift present in the confocal microscopy setup, which explains this movement. To verify this, microbeads on glass were imaged and analyzed (n=54) for their MSDs. The trend of this drift is evident in the analysis (Figure 5c).

When plotting the bead displacements as a function of relative position to the coil, interesting trends emerge (Figure 5b-c). The magnetic microbeads directly below the inner 2 coils move more than those below the outer two. The outer magnetic beads and both groups of nonmagnetic beads do not move more than baseline, suggesting that

outside the inner two turns the magnetic field is having no effect. It is important to note that in all five-minute confocal tests, magnetic and nonmagnetic beads were injected into the same cells. It seems unfeasible that there is direct mechanical coupling of the magnetic beads to the nonmagnetic beads. However, there is a potential for nonmagnetic bead movement due to magnetic bead activity.[9] The average centroid displacement data shows that the beads do not return to their initial position, providing evidence for an active cytoskeletal remodeling due to the forces applied on the beads or possibly demonstrating the viscoelasticity of the cytoplasm. The cytoskeletal remodeling is a global response in a single cell, which could explain the high movement of the nonmagnetic beads in the inner section of the coil. Additionally, while biologically relevant, the microcoil does produce a temperature between 22^{o}C and 25 ^{o}C., increasing the energy of the system. The added heat could explain this subtle increase in background movement. Ultimately, for both the inner and outer sections, the magnetic particles still displace more than the nonmagnetic proving that the magnetic field is still contributing a significant force.

Currently, a few limitations exist with this method. Heat production of the coil is the largest limitation for robustness of this system. Increases the current causes an exponential increase in heat production. The resulting heat causes two problems. First, the heat on the cells themselves is of critical concern. If the current reaches up to even 1mA, the temperature rises to over 100^{o}C, which is unfeasible for biological studies (data not shown, personal communication from Dr. Charilaos Mousoulis). Additionally, the heat causes a larger deflection of the coil moving it further from the sample. Since the

magnetic field is incredibly local with a penetration of a constant field around 30 um (Figure 1d) it is paramount that the system have near zero deflection. Because of temperature and deflection concerns, the magnetic field generation must stay at low femtonewton forces. If the heating issue can be solved, then the magnetic field magnitude range will greatly increase. A potential solution to the heating problem would be a fabricated heat sink. This could be a manufactured channel through the turns of the coil that allow for the flow of a liquid or possibly a sheath that covers the coils allowing for liquid flow. An increase in magnitude could allow for the modeling of cellular response to large displacements and ultimately microrheology models.[24]

Additionally, repeat testing in solutions decreases acceptable contact pad area, making coil reusability difficult. The current manufacturing of the microcoil leaves the contact pads exposed to the air for contact with the nosecone clamps. The open gold seems to degrade away at a rapid pace when introduced to liquid, whether due to the liquid alone or in combination with the heat production by the current through the microcoil, leaving gold only where the nosecone clamps came into contact with the contact pad originally. A simple solution to this would be to thinly coat ($<10\mu$m) the whole microcoil contact pad and AFM nosecone with an insulator such as Parylene-C or Slygard 184, thus allowing no contact between the gold surface and any liquid. Lastly, the differences in microparticles could play a role in the response. The microparticle diameters differed by 0.2μm which could play a role in both passive and active motion. Also, due to the differences composition (embedded Iron Oxide vs. Carboxylate) the

beads also have different heat capacities which would affect their reaction to the addition of heat into the system.

The micro inductor enabled cantilever method opens the door for multiple new directions of research. First, the local probing of single cells in a population allows for a higher testing throughput than the setup of traditional magnetic tweezers by not globally applying the magnetic field to the entire testing dish, thus increasing testing efficiency. This is critical for cell populations that differentiate over time with changing mechanical properties.

Second, magnetic tweezers natural ability to performed measurements in solution allows for long-term testing of pharmacological agents ideal for rare (e.g. stem or cancer) or primary cell populations and the addition of the microinductor enabled cantilever allows all studies to be completed in the same dish resulting in more accurate cell population data. For example, with the micro inductor technique, it would be possible to study the internal mechanics of a cancer cell population as you introduce new drugs into the media or internal mechanics of a stem cell line as it differentiates.

Third, coupled with visualization of localized nuclear architecture through chemical staining, it is possible to track changes in intranuclear biomechanics using deformable image registration to elucidate strain transfer from the cytoplasm and perinuclear regions to the nucleus interior.[25] As nuclear structure and mechanics becomes more important, the AFM microcoil method can lead the way.[26] Finally, the testing setup expands current capabilities of AFM. The addition of local magnetic tweezers allows the simultaneous internal and external (surface) monitoring of

mechanical and topographical measures. As biological mechanotransduction of the extracellular matrix (ECM) through the cytoskeleton to the nucleus are linked together, the ability to study multiple mechanics at the same time could potentially reveal more information about this interconnection and start to fit the puzzle pieces together resulting in progress in treating associated diseases such as cancers and heart failure.[1]

1.5. References

[1] D. E. Ingber, "Mechanobiology and diseases of mechanotransduction.," *Ann. Med.*, vol. 35, no. 8, pp. 564–77, Jan. 2003.

[2] M. L. Rodriguez, P. J. McGarry, and N. J. Sniadecki, "Review on Cell Mechanics: Experimental and Modeling Approaches," *Appl. Mech. Rev.*, vol. 65, no. 6, p. 060801, Oct. 2013.

[3] K. C. Neuman and A. Nagy, "Single-molecule force spectroscopy: optical tweezers, magnetic tweezers and atomic force microscopy.," *Nat. Methods*, vol. 5, no. 6, pp. 491–505, Jun. 2008.

[4] J. R. Moffitt, Y. R. Chemla, S. B. Smith, and C. Bustamante, "Recent advances in optical tweezers.," *Annu. Rev. Biochem.*, vol. 77, pp. 205–28, Jan. 2008.

[5] F. H. C. Crick and A. F. W. Hughes, "The physical properties of cytoplasm," *Exp. Cell Res.*, vol. 1, no. 1, pp. 37–80, Jan. 1950.

[6] B. G. Hosu, K. Jakab, P. Bánki, F. I. Tóth, and G. Forgacs, "Magnetic tweezers for intracellular applications," *Rev. Sci. Instrum.*, vol. 74, no. 9, p. 4158, Aug. 2003.

[7] A. Celedon, C. M. Hale, and D. Wirtz, "Magnetic manipulation of nanorods in the nucleus of living cells.," *Biophys. J.*, vol. 101, no. 8, pp. 1880–6, Oct. 2011.

[8] H.-W. Li, B. V. O. Muir, G. Fichet, and W. T. S. Huck, "Nanocontact Printing: A Route to Sub-50-nm-Scale Chemical and Biological Patterning," *Langmuir*, vol. 19, no. 6, pp. 1963–1965, Mar. 2003.

[9] A. R. Bausch, W. Möller, and E. Sackmann, "Measurement of local viscoelasticity and forces in living cells by magnetic tweezers.," *Biophys. J.*, vol. 76, no. 1 Pt 1, pp. 573–9, Jan. 1999.

[10] A. R. Bausch, F. Ziemann, A. A. Boulbitch, K. Jacobson, and E. Sackmann, "Local measurements of viscoelastic parameters of adherent cell surfaces by magnetic bead microrheometry.," *Biophys. J.*, vol. 75, no. 4, pp. 2038–49, Oct. 1998.

[11] F. J. Alenghat, B. Fabry, K. Y. Tsai, W. H. Goldmann, and D. E. Ingber, "Analysis of cell mechanics in single vinculin-deficient cells using a magnetic tweezer.," *Biochem. Biophys. Res. Commun.*, vol. 277, no. 1, pp. 93–9, Oct. 2000.

[12] M. Tanase, N. Biais, and M. Sheetz, "Magnetic tweezers in cell biology.," *Methods Cell Biol.*, vol. 83, pp. 473–93, Jan. 2007.

[13] C. Gosse and V. Croquette, “Magnetic tweezers: micromanipulation and force measurement at the molecular level.,” *Biophys. J.*, vol. 82, no. 6, pp. 3314–29, Jun. 2002.

[14] C. Wilhelm, F. Gazeau, and J.-C. Bacri, “Rotational magnetic endosome microrheology: Viscoelastic architecture inside living cells,” *Phys. Rev. E*, vol. 67, no. 6, p. 061908, Jun. 2003.

[15] T. E. Lister and P. J. Pinhero, “In Vivo Atomic Force Microscopy of Surface Proteins on Deinococcus radiodurans,” *Langmuir*, vol. 17, no. 9, pp. 2624–2628, May 2001.

[16] N. Jalili and K. Laxminarayana, “A review of atomic force microscopy imaging systems: application to molecular metrology and biological sciences,” *Mechatronics*, vol. 14, no. 8, pp. 907–945, Oct. 2004.

[17] R. Lal and S. A. John, “Biological applications of atomic force microscopy,” *Am J Physiol Cell Physiol*, vol. 266, no. 1, pp. C1–21, Jan. 1994.

[18] A. Vinckier and G. Semenza, “Measuring elasticity of biological materials by atomic force microscopy,” *FEBS Lett.*, vol. 430, no. 1–2, pp. 12–16, Jun. 1998.

[19] S. S. Shevkoplyas, A. C. Siegel, R. M. Westervelt, M. G. Prentiss, and G. M. Whitesides, “The force acting on a superparamagnetic bead due to an applied magnetic field.,” *Lab Chip*, vol. 7, no. 10, pp. 1294–302, Oct. 2007.

[20] J. F. Antaki, “An experimental and theoretical model for the passive biomechanical properties of the intact heart (Volumes I and II),” University of Pittsburgh, 1991.

[21] D. E. J. Anderson and K. A. Athanasiou, “A comparison of primary and passaged chondrocytes for use in engineering the temporomandibular joint.,” *Arch. Oral Biol.*, vol. 54, no. 2, pp. 138–45, Feb. 2009.

[22] F. Ziemann, J. Rädler, and E. Sackmann, “Local measurements of viscoelastic moduli of entangled actin networks using an oscillating magnetic bead micro-rheometer.,” *Biophys. J.*, vol. 66, pp. 2210–2216, 1994.

[23] A. Kishino and T. Yanagida, “Force measurements by micromanipulation of a single actin filament by glass needles.,” *Nature*, vol. 334, no. 6177, pp. 74–6, Jul. 1988.

[24] O. Lunov, S. Bespalova, and V. Zablotskii, “A model for magnetic bead microrheometry,” *J. Magn. Magn. Mater.*, vol. 311, pp. 162–165, 2007.

[25] J. T. Henderson, G. Shannon, A. I. Veress, and C. P. Neu, “Direct measurement of intranuclear strain distributions and RNA synthesis in single cells embedded within native tissue.,” *Biophys. J.*, vol. 105, no. 10, pp. 2252–61, Nov. 2013.

[26] M. Zwerger, C. Y. Ho, and J. Lammerding, “Nuclear mechanics in disease.,” *Annu. Rev. Biomed. Eng.*, vol. 13, pp. 397–428, Aug. 2011.

1.6. Figures

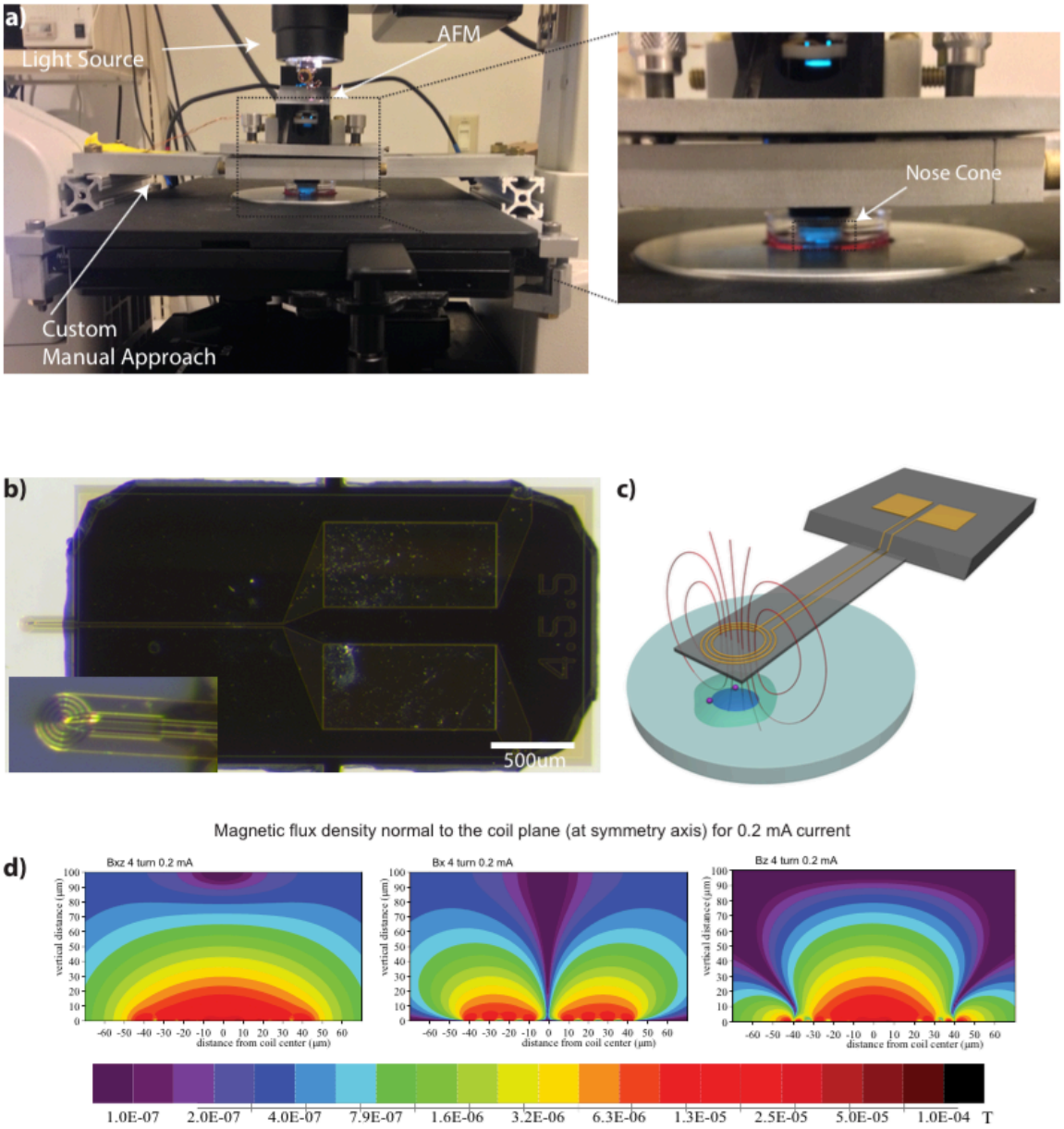

Figure 1. The setup and characterization of the functionalized AFM cantilever and microcoil. a) The overall magnetic manipulation testing setup with custom AFM manual approach. b) A 4 turn microcoil. c) A visual of the testing setup with the magnetic field lines induced by the microcoil affecting the magnetic beads inside the cell. d) The magnetic flux density of the 4 turn microcoil at .2mA.

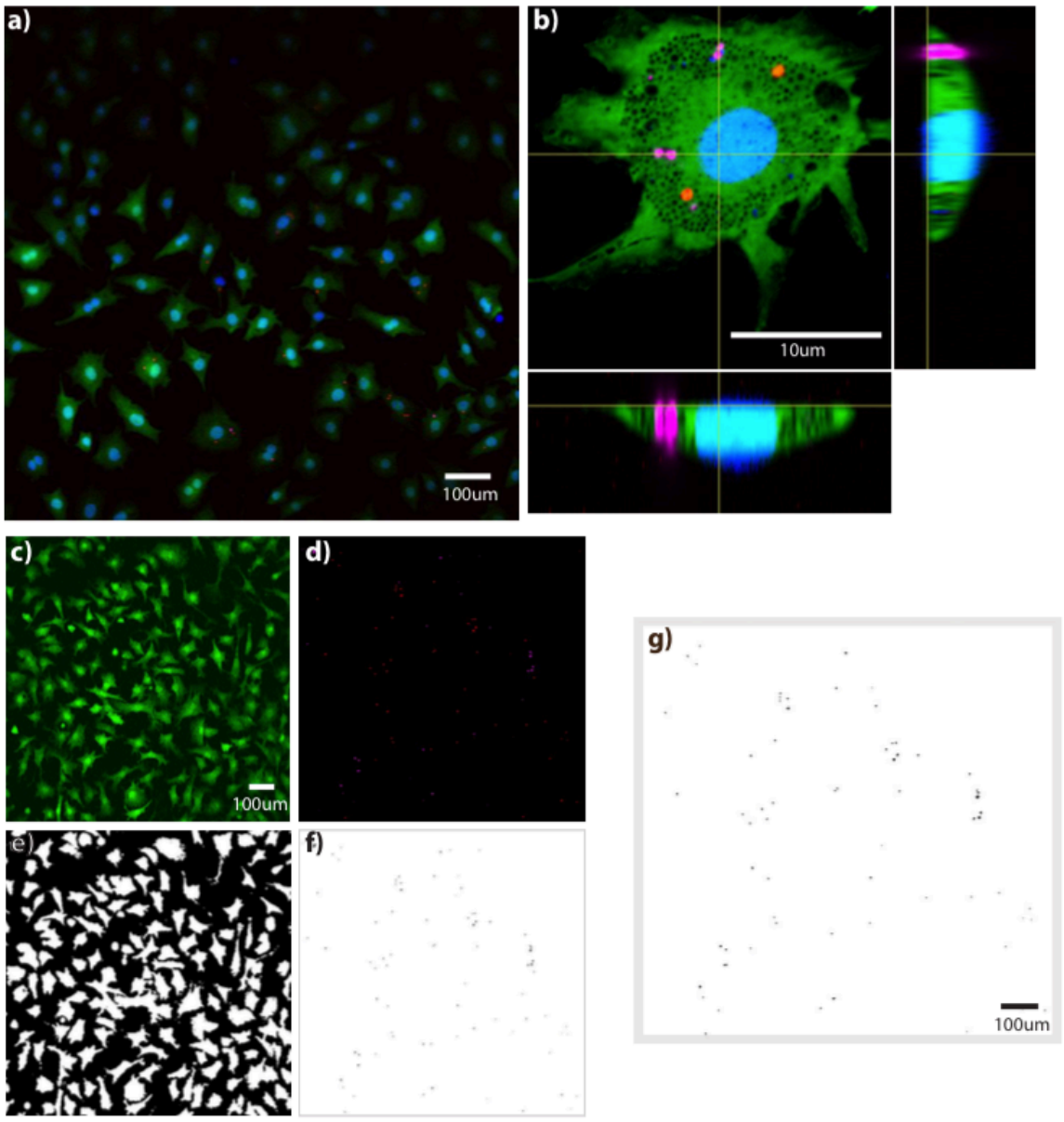

Figure 2. Ballistic Injection Process. a) Images (20×) of plated chondrocytes confirm microinjected superparamagnetic (magenta) and nonmagnetic (red) particles throughout the body (and nucleus of cells: data not shown). b) Confocal image of an injected primary chondrocyte c-d) The original images of the cytoskeletal combined microparticles channels. e-f) The opposite binary images for the cytoskeleton and microparticles channels g) The resulting image subtraction of g-f resulting in the total number of beads injected.

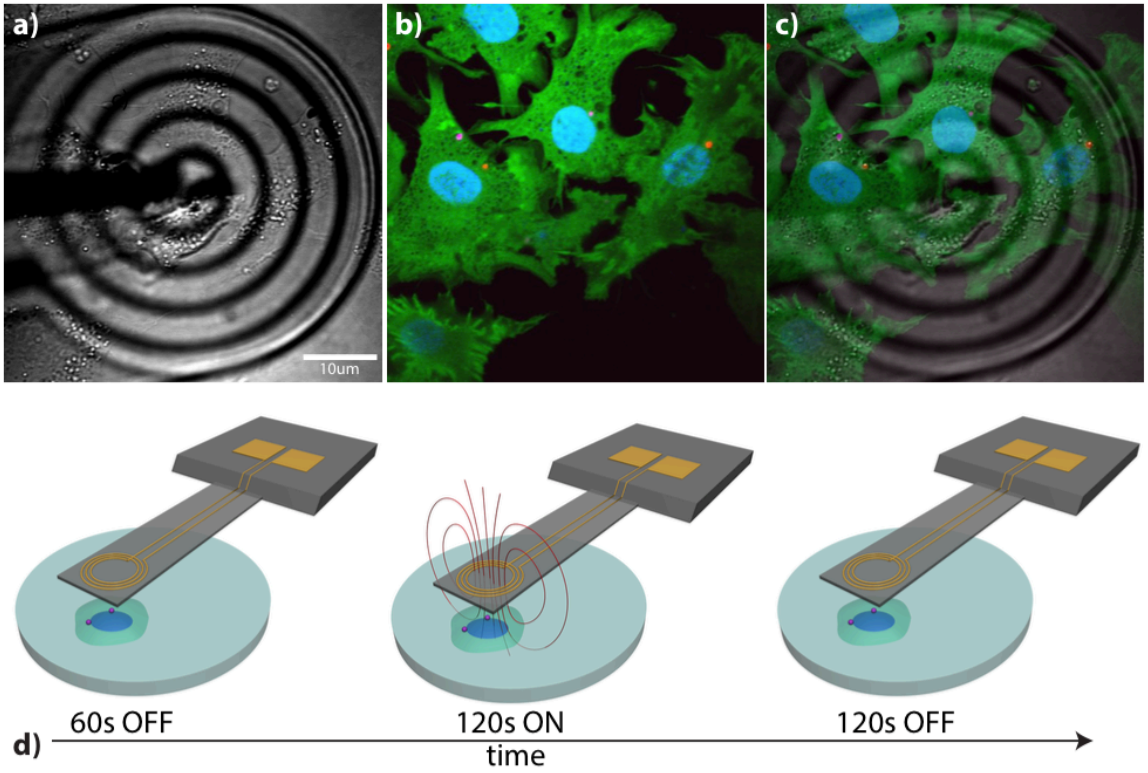

Figure 3. The Magnetic Coil Approach and Manipulation Testing. a-c) A hybrid 4-turn microcoil was positioned 25 μm above the cells. d) The standard 5 minute test. 60s of imaging followed by 120s of pulsing current through the microcoil and completed with another 120s of background imaging.

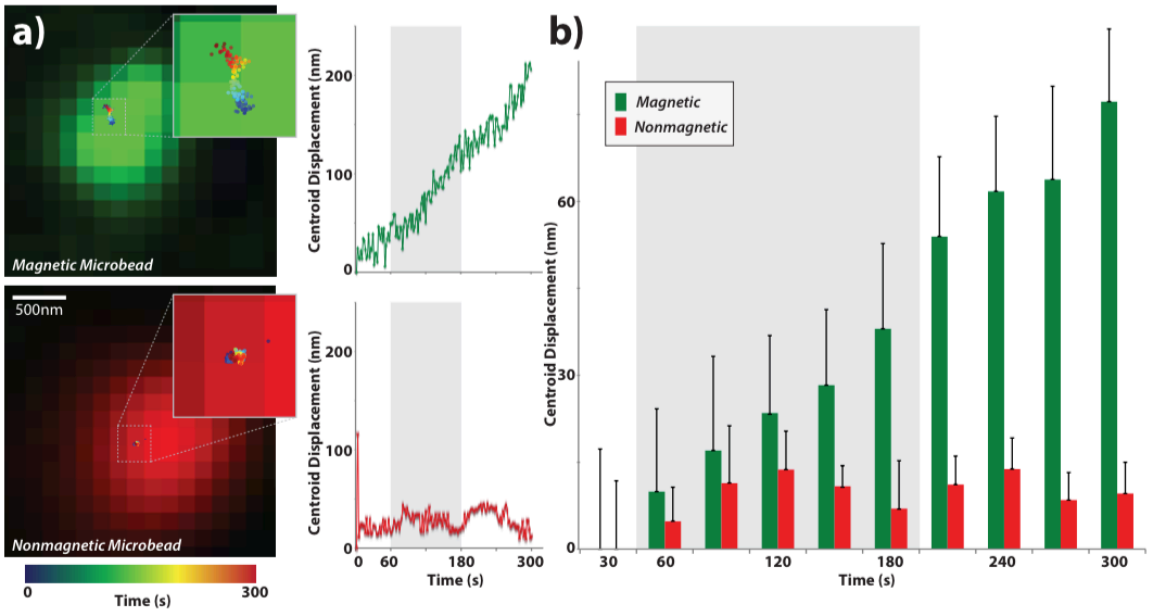

Figure 4. Localized fields from the hybrid probe displace superparamagnetic beads embedded within living cells. a-b). Cyclic magnetic fields (.5s application, 0.1 Hz) applied over two minutes induced nanometer scale displacements of the magnetic bead centroids, compared to controls.

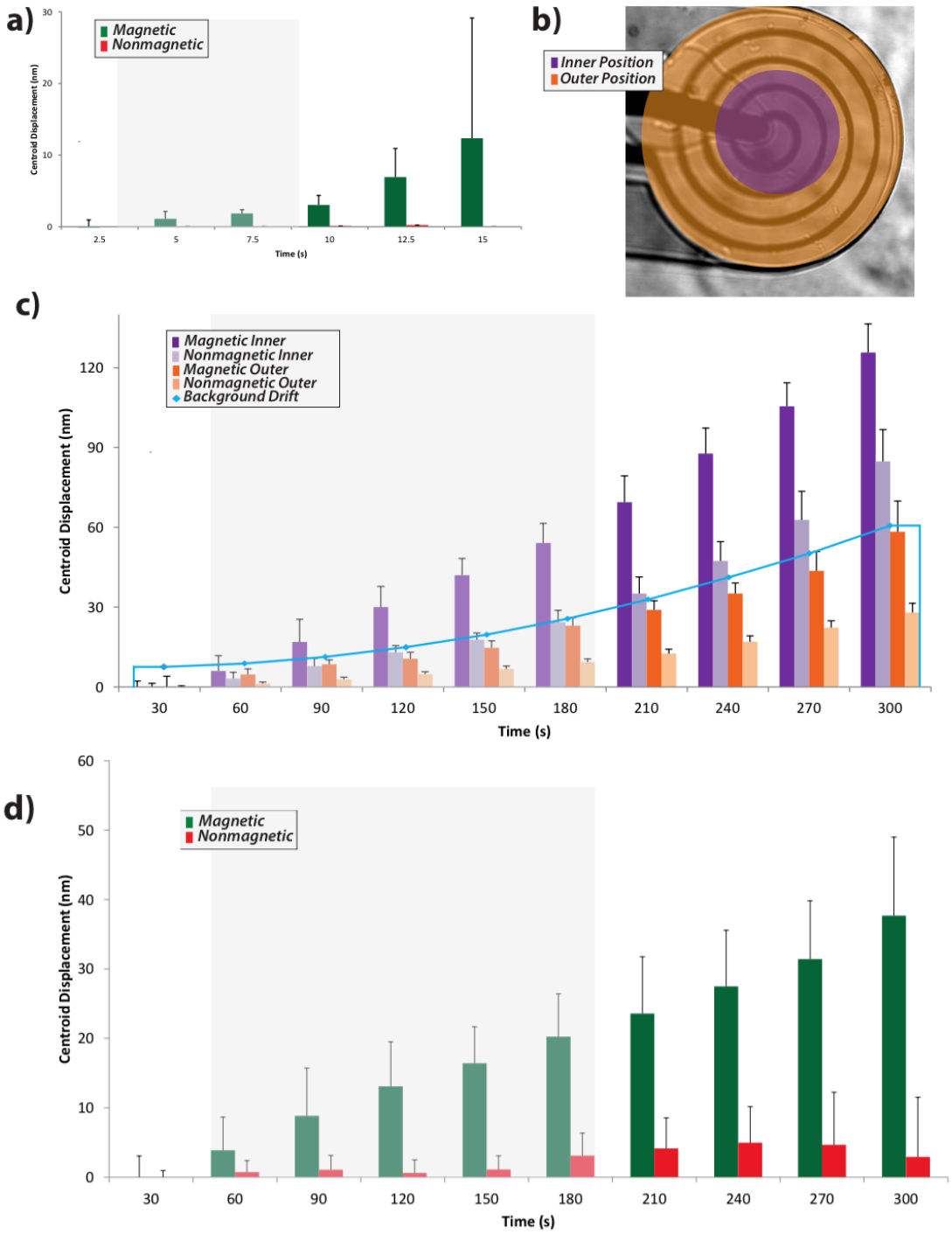

Figure 5. Confocal Analysis Testing. a) 15s tests resulted in a trend of higher displacement of magnetic beads but high variability in the data results in insignificant conclusions. b) The coil positions defined as inner and outer c) Displacements of microparticles relative to microcoil start to explain the variance in data. d) 5 min cyclic magnetic field tests result in displacements similar to those seen using the widefield microscope setting